

## Solvent Exchange Kinetics and Proton Relaxation in Solutions of Cobalt(II) Dioximes

K. Wang and R. B. Jordan\*

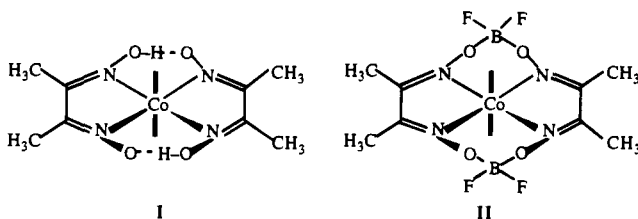
Department of Chemistry, University of Alberta, Edmonton, Alberta, Canada T6G 2G2

Received February 24, 1995<sup>®</sup>

The temperature dependence of the solvent proton transverse and longitudinal relaxation rates has been measured in solutions of the low-spin  $d^7$  complexes of bis(dimethylglyoximate)cobalt(II),  $\text{Co}(\text{dmgH}_2)$ , and bis(diphenylglyoximate)cobalt(II),  $\text{Co}(\text{dpgH})_2$ , in methanol and acetonitrile, and  $\text{Co}(\text{dmgBF}_2)_2$  in acetone and acetonitrile. There is distinct evidence for solvent exchange controlled transverse relaxation in all systems except  $\text{Co}(\text{dpgH})_2$  in acetonitrile. The rate constants are similar in magnitude to those of hexasolvated, high-spin cobalt(II) complexes. However, the cobalt(II) oximes are less favorable for NMR relaxation studies because of their longer electron spin relaxation times, although the chemical shifts are generally larger than those of hexasolvated cobalt(II). The solvent exchange rate constant (25 °C),  $\Delta H^\ddagger$  (kcal mol<sup>-1</sup>),  $\Delta S^\ddagger$  (cal mol<sup>-1</sup> K<sup>-1</sup>) are  $2.3 \times 10^5$ ,  $7.2 \pm 0.2$ ,  $-9.8 \pm 0.7$  for  $\text{Co}(\text{dmgH}_2)$  in acetonitrile,  $2.8 \times 10^4$ ,  $13.9 \pm 0.2$ ,  $8.3 \pm 0.6$  for  $\text{Co}(\text{dmgH}_2)$  in methanol,  $1.4 \times 10^5$ ,  $4.3 \pm 0.3$ ,  $-20.5 \pm 1$  for  $\text{Co}(\text{dmgBF}_2)_2$  in acetonitrile,  $3.5 \times 10^5$ ,  $3.4 \pm 0.9$ ,  $-22 \pm 5$  for  $\text{Co}(\text{dmgBF}_2)_2$  in acetone, and  $1.2 \times 10^6$ ,  $3.4 \pm 0.4$ ,  $-21 \pm 2$  for  $\text{Co}(\text{dpgH})_2$  in methanol.

## Introduction

Since the pioneering work of Schrauzer,<sup>1</sup> cobaloximes have been widely studied as models for coenzyme B<sub>12</sub>. These are bis complexes of dimethylglyoximate ( $\text{dmgH}^-$ , the anion derived from 2,3-butanedione dioxime), as shown in I. There are numerous derivatives in which the methyl groups are replaced by other organic groups, and the O-H-O bridges may be replaced by two BF<sub>2</sub> bridges as in II.



This family of complexes generally mimics coenzyme B<sub>12</sub> by having the cobalt in the I, II, and III oxidation states, corresponding to B<sub>12s</sub>, B<sub>12r</sub>, and B<sub>12</sub>, respectively. The cobalt(III) complexes are the most stable and most widely characterized and studied.<sup>2</sup> They are octahedral, low-spin  $d^6$  complexes with a *trans* arrangement of two additional ligands (X, Y), and most notably they form organometallic derivatives analogous to coenzyme B<sub>12</sub>.

This study is concerned with the cobalt(II) complexes. These are low-spin  $d^7$  systems that typically are fairly easy to oxidize to the cobalt(III) state and have modest solubility in polar solvents. Although the cobalt(II) systems are models of B<sub>12r</sub>, they have not been widely studied, and nothing quantitative is known about their substitution lability.

Solid state structures of cobaloximes(II) are rare due to the air-sensitive nature of the complexes and the difficulty in

obtaining single crystals. The bis(pyridine) adduct,  $(\text{py})_2\text{Co}^{\text{II}}(\text{dmgH}_2)$ ,<sup>3</sup> has the  $(\text{dmgH}_2)$  chelate ring almost coplanar with the Co atom, and the axial Co-N bonds to pyridine (2.25 Å) are 0.36 Å longer than the equatorial Co-N bonds to  $\text{dmgH}^-$  (1.89 Å). The structure of  $(\text{CH}_3\text{OH})_2\text{Co}^{\text{II}}(\text{dmgBF}_2)_2$ <sup>4</sup> also shows axial elongation, with Co-N<sub>eq</sub> and Co-O<sub>ax</sub> (CH<sub>3</sub>OH) bond lengths of 1.88 and 2.26 Å, respectively. The axial elongation can be attributed to the unpaired electron occupying the slightly antibonding  $d_{z^2}$  orbital in these low-spin  $d^7$  complexes.

In solution, cobaloxime(II) may form mono- and bis(Lewis base) adducts. However, the structure of the cobaloxime(II) in solution can be difficult to assess because the axial sites are labile. Depending upon such factors as solvent, nature and concentration of the Lewis base, and the temperature, the  $\text{Co}^{\text{II}}(\text{dmgH}_2)$  moiety in solution may coordinate to one or two axial ligands. In fact, the complex may be 5-coordinate in solution even though it is 6-coordinate in the solid state, and vice versa. The structure may be further complicated if the solvent is a Lewis base and therefore a potential axial ligand.

The extent of coordination has been deduced most often from EPR spectra of frozen solutions. Such studies can provide the most direct indication of the extent of axial coordination in cases where the donor atom of the axial ligand(s) has a nuclear spin. The pattern of superhyperfine coupling between the unpaired electron on the cobalt and the nuclear spin of the donor atom shows whether one or two donor atoms are attached to the cobalt center and therefore gives the axial coordination number. Unfortunately, it is seldom possible to observe isotropic EPR spectra for fluid solutions of cobaloxime(II) complexes, because the electron spin relaxation times are too short, so that the lines are broad. Therefore, EPR spectra are usually measured in frozen solutions at liquid nitrogen temperature (77 K). These spectra reflect the extent of axial coordination in the frozen state, but this may not necessarily be the same as in solution.

Results of EPR measurements on cobaloximes(II) in frozen solutions<sup>4-11</sup> show both 5- and 6-coordinate species. For N-donor Lewis bases, such as pyridine (in methanol)<sup>6,7</sup> and

<sup>®</sup> Abstract published in *Advance ACS Abstracts*, October 1, 1995.

- (1) See, for example: (a) Schrauzer, G. N. *Acc. Chem. Res.* **1968**, *1*, 97. (b) Pratt, J. M. *Inorganic Chemistry of Vitamin B<sub>12</sub>*; Academic: New York, 1972.
- (2) Bresciani-Pahor, N.; Forcolin, M.; Marzilli, L. G.; Randaccio, L.; Summers, M. F.; Toscano, P. J. *Coord. Chem. Rev.* **1985**, *63*, 1. Randaccio, L.; Bresciani-Pahor, N.; Zangrando, E.; Marzilli, L. G. *Chem. Soc. Rev.* **1989**, *18*, 225 and references therein.

(3) Fallon, G. D.; Gatehouse, B. M. *Cryst. Struct. Commun.* **1978**, *7*, 263.

(4) Bakac, A.; Brynildson, M. E.; Espenson, J. H. *Inorg. Chem.* **1986**, *25*, 4108.

(5) Schrauzer, G. N.; Lee, L. P. *J. Am. Chem. Soc.* **1968**, *90*, 6541.

acetonitrile<sup>10</sup>) and 1-methylimidazole (in acetonitrile),<sup>10</sup> mono adducts were generally found at low base concentrations (usually  $[B]/[\text{cobalt}] \leq 1$ ), on the basis of the triplet hyperfine splitting caused by <sup>14</sup>N, while 6-coordinate bis adducts were found at higher base concentrations, as shown by the quintet splitting pattern of <sup>14</sup>N. In frozen acetonitrile, the bis(solvent) adduct  $(\text{CH}_3\text{CN})_2\text{Co}^{\text{II}}(\text{dmgBF})_2$  was observed.<sup>11</sup>

The electronic spectra can be used to determine whether  $\text{Co}(\text{dmgH})_2$  is 5- or 6-coordinate in solution, if the two adducts have distinguishable spectra.<sup>12</sup> However, both this and the EPR method can be ambiguous if the solvent is a Lewis base, because the observation of 1:1 base adduct does not rule out coordination by a solvent in the second axial position to give 6-coordinate (base)(solvent) $\text{Co}^{\text{II}}(\text{dmgH})_2$ .

The present work was undertaken to use NMR to measure the solvent exchange rates of the solvated cobalt(II) complexes, referred to as cobaloximes(II). Although the NMR method has been widely applied, this work is somewhat exploratory because of the lack of information on the NMR relaxation effects and exchange rates for low-spin  $d^7$  systems. Another intention was to use rotating-frame  $T_{1\rho}$  measurements<sup>13</sup> to determine the solvation number of  $\text{Co}^{\text{II}}(\text{dmgH})_2$  in various solvents. This goal has been frustrated by the unfavorable solubility and relaxation properties of the systems, which require that the rotating field must be left on for times that cause serious sample heating and potential probe damage.

**NMR Relaxation Rate Analysis.** The analysis of the transverse relaxation rate ( $R_2$ ) follows the original development by Swift and Connick<sup>14</sup> with the addition of the outer-sphere effect suggested by Luz and Meiboom,<sup>15</sup> and the result is given by eq 1, where  $R_{2\text{obs}}$  is the observed transverse relaxation rate

$$R_{2p} = \frac{1}{P_m}(R_{2\text{obs}} - R_{2\text{solv}}) = nr_m \left[ \frac{R_{2m}(R_{2m} + r_m) + (\Delta\omega_m)^2}{(R_{2m} + r_m)^2 + (\Delta\omega_m)^2} \right] + R_{2o} \quad (1)$$

for the bulk solvent nuclei,  $R_{2\text{solv}}$  is the relaxation rate of the bulk solvent in the absence of chemical exchange,  $r_m$  is the first-order solvent exchange rate constant,  $n$  is the number of exchangeable coordinated solvent molecules in the solvation shell of the metal ion M,  $P_m = [\text{MS}^*_n]/[\text{S}]$  is defined as the ratio of molar concentration of metal ion to that of bulk solvent,  $R_{2m}$  is the transverse relaxation rate of the bound solvent nuclei in the absence of the exchange,  $R_{2o}$  is the outer-sphere relaxation rate,  $\Delta\omega_{\text{obs}}$  is the observed chemical shift of the bulk solvent nuclei in the presence of chemical exchange, and  $\Delta\omega_m$  is the chemical shift of the bound solvent nuclei in the absence of chemical exchange. Both shifts are relative to that of bulk

solvent in the absence of chemical exchange, which is essentially the resonance frequency of the pure solvent.

The observed chemical shift is given by eq 2.

$$\Delta\omega_{\text{obs}} = \frac{nP_m\Delta\omega_m}{(R_{2m}/r_m + 1)^2 + (\Delta\omega_m)^2/r_m^2} \quad (2)$$

The expression for the longitudinal NMR relaxation rate  $R_{1p}$ , which was given by Bloembergen and Morgan<sup>16</sup> and later derived by Luz and Meiboom,<sup>15</sup> is given by eq 3 where the

$$R_{1p} = \frac{1}{P_m}(R_{1\text{obs}} - R_{1\text{solv}}) = \frac{nr_m R_{1m}}{R_{1m} + r_m} + R_{1o} \quad (3)$$

$R_{1o}$ 's are defined analogously to their corresponding  $R_{2o}$ 's. This equation can be obtained from eq 1 by setting  $\Delta\omega_m = 0$  and replacing  $R_{2m}$  and  $R_{2o}$  by  $R_{1m}$  and  $R_{1o}$ , respectively.

The temperature dependence of the terms in the above equations has been discussed previously<sup>17</sup> so that the equations will just be given here to define terms. The inner- and outer-sphere relaxation rates are given by eq 4 where  $i = 1$  or  $2$ ,  $j =$

$$R_{ij} = \frac{C_{ij}}{T} \exp\left(\frac{E_{ij}}{RT}\right) \quad (4)$$

$m$  or  $o$ , and  $C_{ij}$  and  $E_{ij}$  are temperature-independent pre-exponential factors and activation energies, respectively. The temperature dependence of the first-order solvent exchange rate constant  $r_m$  is given by transition state theory, with the activation enthalpy ( $\Delta H^\ddagger$ ) and entropy ( $\Delta S^\ddagger$ ) for the solvent exchange as temperature-independent parameters.

Bloembergen<sup>18</sup> first developed eq 5 to describe the temperature dependence of  $\Delta\omega_m$  and this can be simplified to the form at the right of eq 5, where  $C_\omega$  is a temperature-independent

$$\Delta\omega_m = -\omega_0 \frac{\mu_{\text{eff}} \beta \sqrt{S(S+1)}}{3k_B T \gamma_1} \left(\frac{A}{\hbar}\right) = \frac{C_\omega}{T} \quad (5)$$

constant if  $\mu_{\text{eff}}$  (the effective magnetic moment of the paramagnetic species in solution) is temperature independent and where  $\omega_0$  is the operating frequency of the NMR spectrometer,  $S$  is the electron spin quantum number of the paramagnetic species,  $\gamma_1$  is the magnetogyric ratio of the nucleus being observed,  $k_B$  is the Boltzmann constant, and  $A/\hbar$  ( $\text{s}^{-1}$ ) is the scalar (hyperfine) coupling constant for the interaction between the unpaired electron(s) on the paramagnetic site and the nuclei of the coordinated solvent.

The general temperature dependence of  $R_{2p}$  was described by Swift and Connick<sup>13</sup> with the assumption that  $\Delta H^\ddagger > E_{im} \approx E_{io}$  so that  $r_m$  has a greater temperature dependence than  $R_{2o}$  and  $R_{2m}$  and that  $\Delta\omega_m$  has the smallest temperature dependence, as expected from eq 5. Then, at high temperature (region I), chemical exchange is faster than inner-sphere relaxation ( $r_m^2 \gg R_{2m}^2, R_{2m}r_m$ ) and relaxation is controlled by  $R_{2m}$  and given by eq 6. As the temperature is lowered (region II), the chemical

$$R_{2p} = nR_{2m} + R_{2o} \quad (6)$$

exchange is still fast ( $r_m^2 \gg R_{2m}^2, R_{2m}r_m, (\Delta\omega_m)^2$ ;  $(\Delta\omega_m)^2 \gg R_{2m}^2, R_{2m}r_m$ ) but relaxation is controlled by the dephasing due to the chemical shift difference between the bound and the bulk solvent nuclei and is given by eq 7. At still lower temperature (region III), relaxation is controlled by the rate of chemical exchange ( $(\Delta\omega_m)^2 \gg r_m^2, R_{2m}^2$ ).

- (6) Rockenbauer, A.; Zahonyi, E. B.; Simandi, L. I. *J. Chem. Soc., Dalton Trans.* **1975**, 1729.  
 (7) Rockenbauer, A.; Zahonyi, E. B.; Simandi, L. I. *J. Coord. Chem.* **1972**, 2, 53.  
 (8) Hoshino, M.; Konishi, S.; Terai, Y.; Imamura, M. *Inorg. Chem.* **1982**, 21, 89.  
 (9) De Castro, B.; Rangel, M.; Raynor, J. B. *J. Chem. Soc., Dalton Trans.* **1990**, 3311. Acros, T.; De Castro, B.; Ferreira, M. J.; Rangel, M.; Raynor, J. B. *J. Chem. Soc., Dalton Trans.* **1994**, 369.  
 (10) Lance, K. A.; Goldsby, K. A.; Busch, D. H. *Inorg. Chem.* **1990**, 29, 4537.  
 (11) Unpublished observations: Wang, K. Ph.D. Thesis, University of Alberta, 1994.  
 (12) Simandi, L. I.; Zahonyi, E. B.; Szverenyi, Z.; Nemeth, S. *J. Chem. Soc., Dalton Trans.* **1980**, 276.  
 (13) Chopra, S.; McClung, R. E. D.; Jordan, R. B. *J. Magn. Reson.* **1984**, 59, 361.  
 (14) Swift, T. J.; Connick, R. E. *J. Chem. Phys.* **1962**, 37, 308.  
 (15) Luz, Z.; Meiboom, S. *J. Chem. Phys.* **1964**, 40, 2686.

- (16) Bloembergen, N.; Morgan, L. O. *J. Chem. Phys.* **1961**, 34, 842.  
 (17) Rusnak, L. L.; Jordan, R. B. *Inorg. Chem.* **1976**, 15, 709.  
 (18) Bloembergen, N. *J. Chem. Phys.* **1957**, 27, 595.

$$R_{2p} = n \frac{(\Delta\omega_m)^2}{r_m} + R_{2o} \quad (7)$$

$$R_{2p} = nr_m + R_{2o} \quad (8)$$

Finally in the low-temperature limit (region IV), chemical exchange is slow and relaxation is just determined by the outer-sphere contribution.

For  $R_{1p}$ , chemical shift dephasing is not effective so that region II (eq 7) is not observed. As a consequence,  $R_{1p}$  is given over a much longer temperature range by the equivalent of eq 6 than is the case for  $R_{2p}$ . This also means that  $R_{1p}$  is less useful in determining solvent exchange rates, but it can give more definitive  $E_{ij}$  values, and this is helpful in analyzing the  $R_{2p}$  data.

Measurements of the bulk solvent chemical shift at various temperatures provide an independent method of determining the solvent exchange rate parameters according to eq 2, especially when  $(\Delta\omega_m)^2/r_m^2$  is of the order of 1. In the fast-exchange temperature region where  $r_m^2 \gg R_{2m}^2$ ,  $(\Delta\omega_m)^2$ , eq 2 reduces to eq 9. Thus  $\Delta\omega_m$  can be obtained from the bulk solvent chemical shift measurements in the fast-exchange region.

$$\Delta\omega_{\text{obs}} = nP_m \Delta\omega_m \quad (9)$$

**Dipolar and Scalar Relaxation Mechanisms.** The relaxation rates of the coordinated solvent nuclei,  $R_{im}$ , consist of two contributions from nucleus–electron dipole–dipole and spin–spin interactions called the dipolar ( $R_{iDD}$ ) and scalar ( $R_{iSC}$ ) contributions, respectively. The expressions for  $R_{1m}$  and  $R_{2m}$  have been given by Solomon<sup>19</sup> and Bloembergen.<sup>20</sup> The dipolar term depends on the inverse sixth power of the average electron–nucleus interaction distance ( $r^{-6}$ ) and a correlation time ( $\tau_D$ ); the scalar term depends on the coupling constant ( $A/\hbar$ ) and a correlation time ( $\tau_e$ ).

The correlation times,  $\tau_D$  and  $\tau_e$ , are defined by eqs 10 and 11, where  $\tau_r$  is the rotational correlation time characterizing the tumbling of the metal complex in the solvent,  $\tau_m$  is the average

$$\tau_D^{-1} = \tau_r^{-1} + \tau_m^{-1} + T_e^{-1} \approx \tau_r^{-1} + T_e^{-1} \quad (10)$$

$$\tau_e^{-1} = \tau_m^{-1} + T_e^{-1} \approx T_e^{-1} \quad (11)$$

lifetime of a solvent molecule bound to the metal complex, and  $T_e$  is the electron spin relaxation time<sup>21</sup> of the paramagnetic complex. For small metal complexes in nonviscous solvents,  $\tau_r$  is  $\sim 10^{-11}$  s and in general  $\tau_m \gg \tau_r$ , so that the right-hand approximate forms of eqs 10 and 11 should be valid for the systems of this study. The electron spin relaxation time  $T_e$  may be estimated from the line width of the EPR spectrum of the metal complex. In general, if the solution EPR spectrum can be observed,  $T_e$  must be on the EPR time scale, i.e.,  $T_e > 3 \times 10^{-10}$  s; otherwise  $T_e < 3 \times 10^{-10}$  s.

The relative contributions of  $R_{iDD}$  and  $R_{iSC}$  to the  $R_{im}$  ( $i = 1, 2$ ) can be estimated in terms of the magnitudes of the correlation times  $\tau_D$  and  $\tau_e$ , on the basis of our experimental conditions. It is expected that  $\tau_D$  is controlled by the rotational correlation time  $\tau_r$  (i.e.,  $T_e \gg \tau_r$ ), so that  $\tau_D = \tau_r \approx 1 \times 10^{-11}$  s. Then, the Solomon and Bloembergen equations predict that the relative

dipolar contributions are  $R_{1DD}/R_{2DD} \approx 7/8$ ; i.e., the dipolar contributions for  $R_{1m}$  and  $R_{2m}$  are about the same.

For the scalar contribution, if  $\tau_e = T_e > 10^{-11}$  s, the scalar relaxation equations predict that  $R_{2SC} \gg R_{1SC}$ . Therefore, the difference between the  $R_{2m}$  and  $R_{1m}$  can be attributed to the transverse scalar relaxation rate as given by eq 12. However,

$$R_{2m} - R_{1m} \approx R_{2SC} = \frac{1}{3}S(S+1)\left(\frac{A}{\hbar}\right)^2 T_e \quad (12)$$

if the electron spin relaxation time is very short so that  $T_e \ll \tau_r$ , then both  $\tau_D$  and  $\tau_e$  are controlled by  $T_e$ , and  $R_{1DD} = R_{2DD}$ ,  $R_{1SC} = R_{2SC}$ , and  $R_{1m} = R_{2m}$ , and eq 13 is obtained.

$$R_{2m} = R_{1m} = \left[ \frac{4}{3} \frac{S(S+1)(\gamma_j \beta g)^2}{r^6} + \frac{2}{3} S(S+1) \left(\frac{A}{\hbar}\right)^2 \right] T_e \quad (13)$$

The temperature dependence of  $R_{im}$  is governed by the temperature dependencies of the correlation times  $\tau_r$  and  $\tau_e$ . Assuming  $\tau_r$  and  $\tau_e$  both have an Arrhenius type temperature dependence, then eq 4 is obtained for  $R_{im}$ . Since  $\tau_r$  is related to the solvent viscosity, its activation energy value should be similar to that for the viscosity of pure solvent. However, the temperature dependence of  $T_e$  is the property of the paramagnetic metal complex and could be different from that of  $\tau_r$ . On the other hand,  $T_e$  is also affected by the fluctuation of the micromagnetic field due to the tumbling of the metal complex in solution and  $T_e$  could have an activation energy similar to that of  $\tau_r$ .

The outer-sphere relaxation  $R_{io}$  is due to the interaction of the unpaired electron on the metal complex and protons on solvent molecules in second or higher coordination spheres of the complex. In general, the scalar contribution to the outer-sphere relaxation is considered to be insignificant because the unpaired electron spin density on the metal center is not expected to extend beyond the ligand bound to the metal in the first coordination sphere. In this case, only the dipole–dipole interaction contributes to  $R_{io}$ , and  $R_{1o} \approx R_{2o}$ . However, the scalar relaxation could contribute to the outer-sphere relaxation if the spin density of the unpaired electron(s) on the metal complex can be effectively delocalized through the first coordination sphere ligands onto the solvent nuclei in the second coordination sphere.

Luz and Meiboom<sup>15</sup> have estimated the outer-sphere dipolar relaxation by assuming a spherical shape for the metal complex and averaging the dipole–dipole interaction distance term ( $1/r$ )<sup>6</sup> by integration over the volume between the closest approach of the nuclei in the second coordination sphere, of radius  $d$ , and infinity. The full equation and simplified forms are given in ref 17, where it is also noted that the ratio of the inner- to outer-sphere dipolar contributions is given by eq 14, where  $\rho$

$$\frac{R_{1m}}{R_{1o}} = \frac{3.97 \times 10^2 \left(\frac{d}{r}\right)^3}{\rho S_o} \quad (14)$$

is the solvent density,  $S_o$  is the solvent molality, and the units for  $r$  and  $d$  are angstroms. This ratio is independent of  $\tau_D$ , and eq 14 is useful to estimate either  $R_{1m}$  or  $R_{1o}$  if one of them can be determined experimentally and if values of  $d$  and  $r$  are known.

## Experimental Section

**Materials.** The monosodium salt of dimethylglyoxime, Na(dmGH), was prepared by neutralizing one proton of dimethylglyoxime. Sodium hydroxide (0.38 g,  $9.5 \times 10^{-3}$  mol) was dissolved in  $\sim 3$  mL of distilled water, and then  $\sim 10$  mL of methanol was added. This solution was

(19) Solomon, I. *Phys. Rev.* **1955**, *99*, 559.

(20) Bloembergen, N. *J. Chem. Phys.* **1957**, *27*, 572.

(21) In our treatment, the longitudinal and transverse electron spin relaxation times  $T_{1e}$  and  $T_{2e}$  are assumed to be equal, i.e.,  $T_{1e} = T_{2e} = T_e$ , so that  $\tau_{e1} = \tau_{e2} = \tau_e$ .

added to 60 mL of methanol containing dimethylglyoxime (1.16 g,  $1.0 \times 10^{-2}$  mol). The resulting solution was stirred for 1 h and filtered to remove unreacted dimethylglyoxime. The solvent was removed under reduced pressure, and the yellowish-white solid was washed twice with methanol and dried in vacuum.

The monosodium salt of diphenylglyoxime, Na(dpgH), was prepared by dissolving diphenylglyoxime (2.4 g,  $1.0 \times 10^{-2}$  mol) in ~130 mL of 1,4-dioxane. Then, 10 mL of water containing NaOH (0.38 g,  $9.5 \times 10^{-3}$  mol) was added slowly under stirring. The solution was brought to room temperature and then cooled in ice overnight. Some white crystals precipitated from this solution, and more were obtained by slowly adding 300 mL of hexanes. The product was washed with water several times and dried in air.

Cobalt(II) trifluoromethanesulfonate was prepared by adding trifluoromethanesulfonic acid dropwise to an aqueous suspension of 6.3 g of  $\text{CoCO}_3$  until all the  $\text{CoCO}_3$  dissolved. The solution was filtered and heated to evaporate the water. The light pink solid was recrystallized twice from methanol and dried in vacuum at room temperature, and 15 g of dark pink solid was obtained. The amount of cobalt in the product was determined spectrophotometrically as described below and found to be 12.57%, corresponding to an experimental formula of  $\text{Co}(\text{CF}_3\text{SO}_3)_2 \cdot 3.5\text{CH}_3\text{OH}$ . The cobalt content was constant for more than 2 years, indicating no decomposition to volatile products.

The cobalt was determined by the method of Kitson.<sup>22</sup> A sample containing 0.02 mmol of cobalt was dissolved in 10 mL of water. Then 1.25 g of solid  $\text{NH}_4\text{SCN}$  and 25.00 mL of acetone were added. The solution was brought to 25 °C and diluted to 50.00 mL with water, and the absorbance at 622 nm was recorded. The amount of cobalt was calculated using the molar extinction coefficient of  $1786 \text{ M}^{-1} \text{ cm}^{-1}$ .

The  $\text{Co}(\text{dmgBF}_2)_2 \cdot 2\text{H}_2\text{O}$  was prepared according to the published procedure<sup>23</sup> from  $\text{Co}(\text{OCCH}_3)_2 \cdot 4\text{H}_2\text{O}$  and boron trifluoride etherate in diethyl ether. The brown solid obtained by filtration was washed several times with ice-cold water and methanol and air-dried.

The purity of the  $\text{Co}(\text{dmgBF}_2)_2 \cdot 2\text{H}_2\text{O}$  was checked by chemical analysis and spectroscopy. For the cobalt analysis, 0.018 mmol of  $\text{Co}(\text{dmgBF}_2)_2 \cdot 2\text{H}_2\text{O}$  was dissolved in 15 mL of 1 M NaOH solution and the solution was heated and stirred on a hotplate while 2 mL of 30%  $\text{H}_2\text{O}_2$  solution was added dropwise over 30 min. The solution was brought to 70–85 °C and stirred for 2 h, during which time small portions of water were added to keep the solution volume at about 15 mL. Then the solution was acidified (pH > 2) by slowly adding 2 mL of concentrated HCl. After being boiled for 15 min to destroy any excess  $\text{H}_2\text{O}_2$ , the solution was removed from the hotplate and cooled to room temperature. The cobalt was determined by Kitson's method described above. Anal. Calcd for  $\text{CoC}_3\text{H}_{10}\text{O}_4\text{B}_2\text{F}_4$ : Co, 14.0; C, 14.0; B, 22.8; H, 3.80; N, 13.3. Found: Co, 14.0; C, 23.5; H, 3.76; N, 13.1. Elemental analyses for C, H, and N were performed by the Microanalytical Laboratory of the University of Alberta Chemistry Department.

Electronic spectra of  $\text{Co}(\text{dmgBF}_2)_2$  in various solvents were measured on a Cary 219 spectrophotometer at room temperature. Sample solutions were prepared by adding the solvent, deoxygenated by argon, to a 50-mL volumetric flask containing a weighed amount of  $\text{Co}(\text{dmgBF}_2)_2 \cdot 2\text{H}_2\text{O}$ . The solution was stirred under argon until all the solid dissolved and then transferred with a syringe to an argon-filled 1-cm cuvette sealed with a serum cap. The  $\text{Co}(\text{dmgBF}_2)_2$  solution is much less air sensitive than that of  $\text{Co}(\text{dmgH})_2$ . The air sensitivity somewhat depends on the solvent, with aqueous solutions being the most stable. Thus, for the purpose of UV-vis measurement, aqueous solutions of  $\text{Co}(\text{dmgBF}_2)_2$  could be prepared without deoxygenation. The electronic spectrum of  $\text{Co}(\text{dmgBF}_2)_2$  in water was characterized by the maxima at 454, 326, and 260 nm with molar extinction coefficients of  $4.00 \times 10^3$ ,  $2.08 \times 10^3$ , and  $6.57 \times 10^3 \text{ M}^{-1} \text{ cm}^{-1}$ , respectively. These results are consistent with values of 456, 328, and 260 nm with  $4.06 \times 10^3$ ,  $1.92 \times 10^3$ , and  $5.88 \times 10^3 \text{ M}^{-1} \text{ cm}^{-1}$ , respectively, reported previously.<sup>24</sup> The spectra also were recorded for  $\text{Co}(\text{dmgBF}_2)_2$  in other solvents, and the absorption maxima (in nm)

along with their molar extinction coefficients (in parentheses) are 461 ( $4.11 \times 10^3$ ) and 330 ( $1.92 \times 10^3$ ) in methanol, 425 ( $3.10 \times 10^3$ ) and 328 ( $2.45 \times 10^3$ ) in acetonitrile, and 447 ( $3.41 \times 10^3$ ) in acetone.

For solvents used in NMR experiments, methanol was Mallinckrodt reagent containing 0.013% water, acetonitrile was Anachemia reagent containing 0.3% water, and acetone was Fisher Scientific reagent containing less than 0.05% water. All solvents were dried under vacuum over 4-Å molecular sieves (British Drug House) for at least 24 h before use. Other reagents and sources: dimethylglyoxime, *p*-dimethoxybenzene, Kodak; diphenylglyoxime,  $\text{CF}_3\text{SO}_3\text{H}$ ,  $\text{BF}_3 \cdot \text{OEt}_2$ , Aldrich; 1,4-dioxane, Caledon;  $\text{CoCO}_3$ , Allied Chemical;  $\text{Co}(\text{OCCH}_3)_2 \cdot 4\text{H}_2\text{O}$ , cyclohexane, Fisher Scientific.

**Sample Preparation.**  $\text{Co}(\text{dmgH})_2$  is especially sensitive to dioxygen and must be prepared anaerobically. The solvent was dried over 4-Å molecular sieves under vacuum and degassed by at least two freeze-pump-thaw cycles on a vacuum line. Then 12–15 mL of the solvent was vacuum-distilled into a preweighed bottle containing weighed amounts of  $\text{Co}(\text{CF}_3\text{SO}_3)_2 \cdot 3.5\text{CH}_3\text{OH}$  (12.57% Co) and a slight stoichiometric excess of Na(dmgH). The bottle was weighed again to determine the weight of the solvent transferred. The resulting yellow-orange solution was transferred under vacuum to a 10-mm flat-bottomed NMR tube (Wilma Glass Co.), which was then sealed under vacuum. The molar concentration of the  $\text{Co}(\text{dmgH})_2$  complex in each sample solution was calculated from the weights of cobalt and solvent and the density of the solvent.  $\text{Co}(\text{dpgH})_2$  samples were prepared in the same way from  $\text{Co}(\text{CF}_3\text{SO}_3)_2 \cdot 3.5\text{CH}_3\text{OH}$  and Na(dpgH). For  $\text{Co}(\text{dmgBF}_2)_2$  samples, the solvent was distilled onto preweighed solid  $\text{Co}(\text{dmgBF}_2)_2 \cdot 2\text{H}_2\text{O}$ .

**NMR Relaxation Rate Measurements.** A Bruker SXP pulse spectrometer operating at 89.5 MHz was used.<sup>25</sup> Pulses were generated and data collected with a Nicolet Instrument Corp. Model 1180 computer and 293A programmable pulser. Relaxation rate data were collected and analyzed by using programs developed in these laboratories. The sample volume ( $0.8\text{--}1.2 \text{ cm}^3$ ) was less than that of the  $\text{H}_1$  coil to minimize the  $\text{H}_1$  field inhomogeneity. Temperature was controlled by a Bruker B-ST 100/700 temperature control unit for above-room-temperature measurements. For low-temperature measurements, a stream of nitrogen gas, cooled by either methanol-dry ice or liquid nitrogen, passed through the NMR probe. Temperature was measured before and after each set of experiments with a copper-constantan thermocouple inserted into the corresponding solvent contained in an NMR sample tube. The stability of the temperature was  $\pm 0.5$  °C over the typical recording time of 0.5–2 h.

Longitudinal relaxation rates ( $R_1$ ) were measured by the standard  $180^\circ\text{--}\tau\text{--}90^\circ$  pulse sequence by using 15–18  $\tau$  values in the range  $0.8\text{--}3.5T_1$  ( $T_1$  is the longitudinal relaxation time,  $T_1 = 1/R_1$ ). The delay time between each measurement was at least  $5T_1$ . Data were analyzed by standard least-squares methods to a single-exponential decay, and the reported values are the average of five replicate measurements, with a typical standard deviation of less than 2%.

Transverse relaxation rates ( $R_2$ ) were measured by the Carr-Purcell-Meiboom-Gill (CPMG) pulse sequence.<sup>26</sup> At least 200 echoes were collected under computer control, and the data were analyzed by a least-squares method. The typical  $t_{cp}$ , which is the time interval between the pulses in the CPMG experiment, is 0.2–0.6 ms. The reported  $R_2$  values were the average of at least five replicate determinations, with a standard deviation of less than 5%.

**Shift Measurements.** Samples of more concentrated  $\text{Co}(\text{dmgH})_2$  solutions for shift measurements were prepared as described above. In each case, the  $\text{Co}(\text{dmgH})_2$  solution was transferred under vacuum to a standard 5-mm NMR tube (Wilma Glass) containing an internal standard. The standards were *p*-dimethoxybenzene for acetonitrile and cyclohexane for methanol. The chemical shift of the solvent proton relative to internal standards was recorded on a Bruker AM 300 MHz spectrometer at 35 °C.

## Results

The temperature dependence of the solvent proton relaxation rates  $R_{1\text{obs}}$  and  $R_{2\text{obs}}$  were measured for the cobaloxime(II)

(22) (a) Kitson, R. E. *Anal. Chem.* **1950**, *22*, 664. (b) Kupferschmidt, W. C. H. Ph.D. Thesis, University of Alberta, 1982; p 37.

(23) Bakac, A.; Brynildson, M. E.; Espenson, J. H. *Inorg. Chem.* **1986**, *25*, 4108.

(24) Bakac, A.; Espenson, J. H. *J. Am. Chem. Soc.* **1984**, *106*, 5197.

(25) Grant, M.; Jordan, R. B. *Inorg. Chem.* **1981**, *20*, 55.

(26) Meiboom, S.; Gill, D. *Rev. Sci. Instrum.* **1958**, *29*, 688.

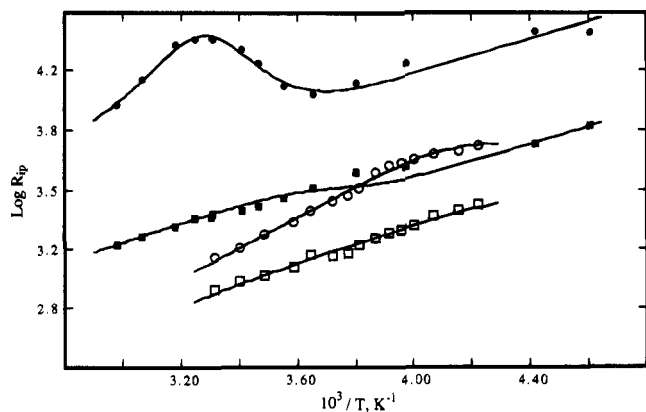


**Figure 1.** Temperature dependence of solvent proton relaxation rates for  $\text{Co}(\text{dmgH})_2$  in acetonitrile ( $P_m = 2.73 \times 10^{-4}$ ,  $R_{2p}$ ,  $\circ$ ,  $R_{1p}$ ,  $\square$ ) and in methanol ( $P_m = 1.21 \times 10^{-4}$ ,  $R_{2p}$ ,  $\bullet$ ,  $R_{1p}$ ,  $\blacksquare$ ). The curves are calculated with parameters in Table 1.

complexes of dimethylglyoxime ( $\text{Co}(\text{dmgH})_2$ ), diphenylglyoxime ( $\text{Co}(\text{dpgH})_2$ ), and the  $\text{BF}_2$  adduct ( $\text{Co}(\text{dmgBF}_2)_2$ ) in several solvents. The  $R_{i\text{obs}}$  data were corrected for pure solvent relaxation,<sup>27</sup> normalized by  $P_m$  according to eqs 1 and 3, and then the temperature dependence was analyzed by least-squares to determine as many as possible of the parameters  $\Delta H^\ddagger$  and  $\Delta S^\ddagger$  for solvent exchange and  $C_{1m}$ ,  $C_{1o}$ ,  $E_{1m}$ ,  $E_{1o}$ , and  $|C_\omega|$ . Since there is uncertainty about the solvation number of these complexes in solutions, a solvation number  $n = 1$  has been assumed. If  $n = 2$ , then the values of  $C_{1m}$ ,  $C_\omega$ , and the solvent exchange rates would decrease by a factor of 2, and  $\Delta S^\ddagger$  would decrease by  $R \ln 2 \approx 1.38 \text{ cal mol}^{-1} \text{ K}^{-1}$ . The parameter  $C_{1o}$  does not depend on the value of  $n$  according to eqs 1 and 3. The solvent NMR shifts could be measured in some cases to provide an independent value of  $C_\omega$ ; however the measured shifts are small because of the limited solubility of the cobaloximes.

**$\text{Co}(\text{dmgH})_2$  in Acetonitrile.** The temperature dependence of solvent proton relaxation rates for this system were measured from  $-43$  to  $+35$  °C, and the  $\log R_{ip}$  vs  $1/T$  plots are shown in Figure 1. From the previous discussion, the  $\log R_{2p}$  curve shows limiting regions I, II, and III corresponding to eqs 6, 7, and 8. The outer-sphere region IV cannot be observed above the freezing point of the solvent. The  $\log R_{1p}$  vs.  $1/T$  curve is close to a straight line and is not sensitive to the solvent exchange, as expected from eq 3 when  $r_m \gg R_{1m}$ , since then  $R_{1p} \approx R_{1m} + R_{1o}$ .

In order to analyze the temperature dependence of the  $R_{ip}$  data, it was assumed that  $R_{1m}$  and  $R_{1o}$  have the same temperature dependence, so that  $E_{1m} = E_{1o}$ . The value of  $E_{1m}$  or  $E_{1o}$  can be determined from the slope of the  $\log R_{1p}$  plot in Figure 1. Then, the value of  $C_{1o}$  is calculated from the estimated  $E_{1o}$  value and the Luz and Meiboom<sup>15</sup> equation, by using  $d = 5.3 \text{ \AA}$  and  $\tau_r = \tau_D = 6.2 \times 10^{-11} \text{ s}$  as determined in a previous study on low-spin  $\text{Co}(\text{trans-[14]diene})^{2+}$  in acetonitrile.<sup>17</sup> Then least-squares fitting of  $R_{1p}$  and  $R_{2p}$  data together was performed by fixing  $C_{1o}$  at the calculated value and setting  $E_{2m} = E_{2o} = E_{1m} = E_{1o}$ ,  $C_{2o} = C_{1o}$ , and  $C_{2m} = C_{1m}$  to yield  $\Delta H^\ddagger$ ,  $\Delta S^\ddagger$ ,  $C_{1m}$ ,  $E_{1m}$ , and  $|C_\omega|$ . The fitting was repeated by adjusting the  $C_{1o}$  value until the most self-consistent parameters were obtained. The best-fit parameters and the calculated  $|A/\hbar|$  and  $T_e$  values are listed in Table 1, and these give the calculated curves in Figure 1.

A solvent proton paramagnetic shift of  $-0.019 \pm 0.0024 \text{ ppm}$  relative to that of pure solvent was measured at 300 MHz and 35 °C in a solution with  $P_m = 9.55 \times 10^{-4}$ . This shift was converted to the operating frequency of 89.5 MHz for the relaxation rate measurements. The shift value was used to calculate  $C_\omega$  and then the scalar coupling constant  $A/\hbar$ . The result (Table 1) shows that the  $C_\omega$  value is in good agreement with that from the  $R_{2p}$  fit.

**$\text{Co}(\text{dmgH})_2$  in Methanol.** The relaxation rates were measured for this system from  $-89$  to  $+60$  °C and are plotted in Figure 1. The  $\log R_{2p}$  curve shows regions II, III, and IV. The extreme-fast-exchange region I, where the relaxation is controlled by  $R_{1m}$ , is not well-defined. In the lowest temperature outer-sphere region (IV), the  $R_{2p}$  and  $R_{1p}$  plots are parallel, indicating that  $E_{1o} \approx E_{2o}$ . The difference in magnitude of  $R_{2p}$  and  $R_{1p}$  in this region is attributed to some outer-sphere scalar relaxation contribution to  $R_{2p}$ .

The  $R_{ip}$  data were analyzed first by assuming that  $E_{1o} \approx E_{1m}$  and that both  $R_{1m}$  and  $R_{1o}$  are due to dipolar relaxation. Taking  $r = 4.8 \text{ \AA}$  and  $d = 9.4 \text{ \AA}$  from the methanol methyl proton results for  $\text{Co}(\text{trans-[14]diene})^{2+}$  in  $\text{CH}_3\text{OH}$ ,<sup>17</sup> one can use eq 14 to calculate the ratio  $C_{1m}/C_{1o} \approx 0.5$ . Then, by assuming  $E_{1m} = E_{2m} = E_{1o} = E_{2o}$  and  $C_{1m} = 0.5C_{1o}$ ,  $R_{1p}$  and  $R_{2p}$  were fitted to yield  $\Delta H^\ddagger$ ,  $\Delta S^\ddagger$ ,  $C_{2m}$ ,  $E_{1m}$ ,  $C_{1o}$ ,  $C_{2o}$ , and  $|C_\omega|$ . The best-fit results are listed in Table 1 and are shown by the calculated curves in Figure 1.

The solvent paramagnetic shifts of the methyl and hydroxyl protons were measured as  $+0.032$  and  $+0.030 \text{ ppm}$ , respectively, at 300 MHz and 35 °C in a solution with  $P_m = 5.90 \times 10^{-4}$ . The magnitudes of  $C_\omega$  and the scalar coupling constant calculated from the paramagnetic shifts agree well with those obtained from the  $R_{2p}$  fit in Table 1.

**$\text{Co}(\text{dmgBF}_2)_2$  in Acetonitrile.** The relaxation rates for this system were measured from  $+26$  to  $-40$  °C and are plotted in Figure 2. The solvent exchange region is apparent as a slight leveling of the  $R_{2p}$  plot at low temperatures but is also evident from the difference between  $R_{2p}$  and  $R_{1p}$ . The analysis of  $R_{ip}$  data was similar to that for  $\text{Co}(\text{dmgH})_2\text{-CH}_3\text{CN}$ . The best-fit parameters are listed in Table 1 and shown by the calculated curves in Figure 2.

The paramagnetic shift of the solvent for a concentrated sample solution of  $P_m = 2.12 \times 10^{-4}$  for this system is only  $\sim 0.003 \text{ ppm}$  and is not reliable since the shift is at the resolution limit of the NMR spectrometer. Nonetheless, the very small paramagnetic shift observed is consistent with the shift of only  $\sim 0.0012 \text{ ppm}$  at 300 MHz and 35 °C predicted from eqs 5 and 9 by using the  $|C_\omega|$  value from Table 1 and the  $P_m$  value for this sample.

**$\text{Co}(\text{dmgBF}_2)_2$  in Acetone.** Acetone was chosen as a solvent because the complex is more soluble in acetone than in methanol. Since the relaxation rate of acetone was not available, the relaxation rate  $R_1$  of pure acetone solvent was measured from  $-90$  to  $+25$  °C. The data<sup>12</sup> are fitted well by the equation  $R_1 = (C/T) \exp(E/RT)$ , with  $C = 1.63 \pm 0.30 \text{ s}^{-1} \text{ K}$  and  $E = 1.375 \pm 0.082 \text{ kcal mol}^{-1}$ .

The relaxation rates for this system were measured from  $-92$  to  $+26$  °C and corrected for pure solvent relaxation, and the  $R_{ip}$  plots are shown in Figure 2. The  $R_{2p}$  plot is similar to that of  $\text{Co}(\text{dmgBF}_2)_2\text{-CH}_3\text{CN}$  in Figure 2. However, the solvent exchange region is less well defined because of the smaller difference between  $R_{2p}$  and  $R_{1p}$ .

Quantitative analysis was started by assuming  $E_{1m} = E_{1o}$  and estimating  $E_{1m}$  from the  $R_{1p}$  data. Estimation of either  $C_{1m}$  or  $C_{1o}$  is complicated here because neither  $d$  nor  $r$  values for acetone are available. However,  $r$  can be approximated by using

(27) Temperature dependences of the relaxation rate  $R_i$  ( $i = 1, 2$ ) for pure  $\text{CH}_3\text{CN}$  and  $\text{CH}_3\text{OH}$  are as follows:  $R_i = (0.0057) \exp(1440/RT)$  for  $\text{CH}_3\text{CN}$ ;  $R_i = (1.463/T) \exp(1801/RT)$  for  $\text{CH}_3\text{OH}$  (Rusnak, L. L. Ph.D. Thesis, University of Alberta, 1971).

**Table 1.** Least-Squares Best-Fit Parameters for the Temperature Dependence of the Solvent Proton Relaxation Rates of Cobalt(II) Dioximes

param <sup>a</sup>	complex, solvent				
	Co(dmgH) <sub>2</sub> , acetonitrile	Co(dmgH) <sub>2</sub> , methanol	Co(dmgBF <sub>2</sub> ) <sub>2</sub> , acetonitrile	Co(dmgBF <sub>2</sub> ) <sub>2</sub> , acetone	Co(dpgH) <sub>2</sub> , methanol <sup>g</sup>
$\Delta H^\ddagger$	7.24 ± 0.19	13.9 ± 0.24	4.33 ± 0.26	3.38 ± 0.90	3.35 ± 0.42 (2.78, 3.81)
$\Delta S^\ddagger$	-9.76 ± 0.73	8.30 ± 0.64	-20.5 ± 0.95	-21.8 ± 4.75	-20.5 ± 2.0 (-23.7, -18.0)
$k^b$	2.3 × 10 <sup>5</sup>	2.8 × 10 <sup>4</sup>	1.4 × 10 <sup>5</sup>	3.5 × 10 <sup>5</sup>	7.2 × 10 <sup>5</sup> (3.9, 12)
$C_{1m}$	(1.42 ± 0.28) × 10 <sup>4</sup>	$C_{10}/2$	(5.88 ± 1.14) × 10 <sup>3</sup>	(3.25 ± 0.93) × 10 <sup>3</sup>	$C_{10}/2$
$C_{2m}$	$C_{1m}$	(7.74 ± 2.31) × 10 <sup>4</sup>	$C_{1m}$	(4.02 ± 1.41) × 10 <sup>3</sup>	5.0 × 10 <sup>3</sup> (0.66, 8.0) <sup>c</sup>
$E_{im} = E_{io}$	1.32 ± 0.07	1.76 ± 0.10	2.12 ± 0.08	1.82 ± 0.05	2.61 ± 0.14 (2.60, 2.54)
$C_{10}$	5.0 × 10 <sup>3</sup> <sup>c</sup>	(2.55 ± 0.45) × 10 <sup>4</sup>	1.30 × 10 <sup>3</sup> <sup>c</sup>	5.0 × 10 <sup>3</sup> <sup>c</sup>	(1.30 ± 0.44) × 10 <sup>3</sup> (1.3, 1.5)
$C_{20}$	5.0 × 10 <sup>3</sup> <sup>c</sup>	(1.03 ± 0.22) × 10 <sup>5</sup>	1.30 × 10 <sup>3</sup> <sup>c</sup>	5.0 × 10 <sup>3</sup> <sup>c</sup>	(1.30 ± 0.44) × 10 <sup>3</sup>
$ C_\omega ^d$	(3.38 ± 0.08) × 10 <sup>6</sup>	(1.13 ± 0.06) × 10 <sup>7</sup>	(2.40 ± 0.10) × 10 <sup>6</sup>	(1.32 ± 0.20) × 10 <sup>6</sup>	(7.55 ± 0.85) × 10 <sup>6</sup> (8.2, 6.7)
$ A/\hbar ^d$	4.76 × 10 <sup>6</sup>	1.60 × 10 <sup>7</sup>	3.39 × 10 <sup>6</sup>	1.87 × 10 <sup>6</sup>	1.07 × 10 <sup>7</sup> (1.16, 0.95)
$T_e^e$	<1.5 × 10 <sup>-11</sup>	6.6 × 10 <sup>-11</sup>	<4.8 × 10 <sup>-11</sup>	6.4 × 10 <sup>-11</sup>	4.2 × 10 <sup>-11</sup>
$C_{if}^f$	-3.5 × 10 <sup>6</sup>	+1.0 × 10 <sup>7</sup> (CH <sub>3</sub> ), +9.6 × 10 <sup>6</sup> (OH)			
$A/\hbar^f$	-4.9 × 10 <sup>6</sup>	+1.5 × 10 <sup>7</sup> (CH <sub>3</sub> ), +1.4 × 10 <sup>7</sup> (OH)			

<sup>a</sup> Units:  $\Delta H^\ddagger$ , kcal mol<sup>-1</sup>;  $\Delta S^\ddagger$ , cal mol<sup>-1</sup> K<sup>-1</sup>;  $k$ , s<sup>-1</sup>;  $C_{1m}$ ,  $C_{2m}$ ,  $C_{10}$ ,  $C_{20}$ , s<sup>-1</sup> K;  $E_{im}$ ,  $E_{io}$ , kcal mol<sup>-1</sup>;  $C_\omega$ , s<sup>-1</sup> K;  $A/\hbar$ , s<sup>-1</sup>;  $T_e$ , s. Error limits are one standard deviation; extra figures, beyond those indicated by error limits, are included to avoid round-off errors in recalculations. <sup>b</sup> First-order solvent exchange rate constant at 25 °C, calculated from  $\Delta H^\ddagger$  and  $\Delta S^\ddagger$  given. <sup>c</sup> Value fixed during least-squares analysis. <sup>d</sup> Determined from fitting the  $R_{2p}$  data;  $A/\hbar$  is calculated from  $C_\omega$ . <sup>e</sup> Estimated at 25 °C by eq 12 from  $R_{2m} - R_{1m}$ ; upper limits assume that this difference is one standard deviation of  $C_{1m}$  or  $C_{2m}$ . <sup>f</sup> Calculated from the measured chemical shift at 300 MHz and 35 °C. <sup>g</sup> Parameters in parentheses are values when  $C_{2m}$  is fixed at 660 or 8.0 × 10<sup>3</sup>, respectively.

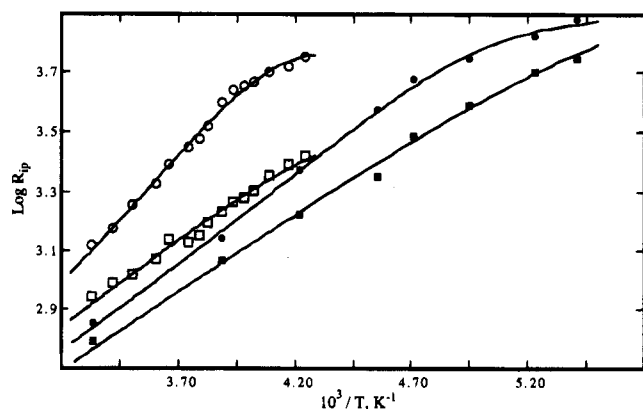


**Figure 2.** Temperature dependence of solvent proton relaxation rates for Co(dmgBF<sub>2</sub>)<sub>2</sub> in acetonitrile ( $P_m = 2.42 \times 10^{-4}$ ,  $R_{2p}$ , ○,  $R_{1p}$ , □) and in acetone ( $P_m = 5.22 \times 10^{-4}$ ,  $R_{2p}$ , ●,  $R_{1p}$ , ■). The curves are calculated with parameters in Table 1.

the bond lengths and angles of the acetone molecule, taking the angle Co-O-C = 130°<sup>28</sup> and the Co-O bond length as 2.3 Å.<sup>29</sup> An average  $r$  value of 4.7 Å is estimated for the methyl protons of acetone by simple geometry. Since acetone and acetonitrile have similar viscosities at 25 °C,<sup>30</sup> it is reasonable to assume that  $\tau_r (= \tau_D)$  in acetone will be the same as that for Co(*trans*-[14]diene)<sup>2+</sup> in CH<sub>3</sub>CN.<sup>16</sup> The dipolar  $R_{1m}$  value at 25 °C can be estimated, and the difference between the observed  $R_{1p}$  and the calculated  $R_{1m}$  at 25 °C is attributed to  $R_{10}$ . Then  $C_{10}$  can be calculated since  $E_{10} (= E_{1m})$  has been evaluated already. The rest of the analysis is similar to that described for Co(dmgH)<sub>2</sub>-CH<sub>3</sub>CN except that it was not necessary to fix  $C_{2m}$  equal to  $C_{1m}$  during the fitting. The final results are given in Table 1, and the calculated curves are shown in Figure 2.

The solvent paramagnetic shift for a sample with  $P_m = 6.60 \times 10^{-4}$  at 35 °C is only ~0.0025 ppm at 300 MHz. This shift, like that in Co(dmgBF<sub>2</sub>)<sub>2</sub>-CH<sub>3</sub>CN, is too small to be reliable

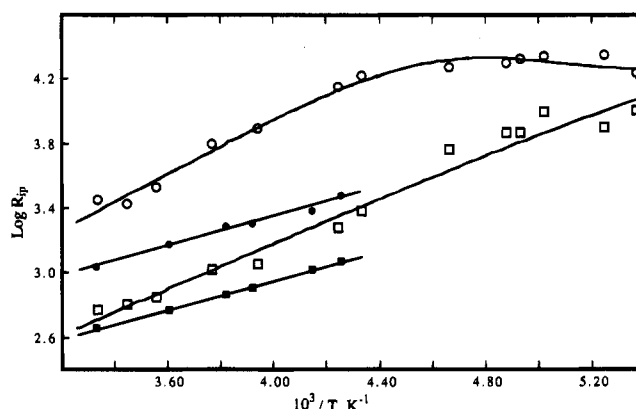


**Figure 3.** Temperature dependence of solvent proton relaxation rates for Co(dpgH)<sub>2</sub> in methanol ( $P_m = 1.82 \times 10^{-4}$ ,  $R_{2p}$ , ○,  $R_{1p}$ , □) and in acetonitrile ( $P_m = 3.88 \times 10^{-4}$ ,  $R_{2p}$ , ●,  $R_{1p}$ , ■). The curves are calculated with parameters in Table 1 for methanol ( $C_{2m}$  fixed at 5.0 × 10<sup>3</sup> s<sup>-1</sup> K) and in the text for acetonitrile.

but is consistent with a shift value of only 0.0016 ppm predicted for this sample by the  $|C_\omega|$  in Table 1.

**Co(dpgH)<sub>2</sub> in Acetonitrile.** The log  $R_{2p}$  plot for this system in Figure 3 is just a straight line with no indication of a solvent exchange region. This could be attributed to either fast exchange in region I with inner-sphere relaxation  $R_{2m}$  or slow exchange in region IV with outer-sphere relaxation  $R_{20}$ . The  $R_{1p}$  and  $R_{2p}$  data were fitted separately by the equation  $R_{ip} = (C_i/T) \exp(E_i/RT)$ . As expected, the  $E_1$  and  $E_2$  values of 1.49 ± 0.05 and 1.46 ± 0.12 kcal mol<sup>-1</sup> are essentially equal. The  $C_1$  and  $C_2$  values are (1.11 ± 0.12) × 10<sup>4</sup> and (2.95 ± 0.72) × 10<sup>4</sup> s<sup>-1</sup> K, respectively.

In order to determine if the system is in region I or IV, values of  $R_{1m}$  and  $R_{10}$  at 298 K were calculated using the  $d$ ,  $r$ , and  $\tau_r (= \tau_D)$  values for Co(*trans*-[14]diene)<sup>2+</sup> in CH<sub>3</sub>CN.<sup>17</sup> These estimates give  $R_{1m} = 4.0 \times 10^2$  s<sup>-1</sup> and  $R_{10} = 1.6 \times 10^2$  s<sup>-1</sup>, compared to the experimental value of 4.6 × 10<sup>2</sup> s<sup>-1</sup>. Therefore it appears that the system is in region I, where exchange is fast and the relaxation is controlled by  $R_{im} + R_{io}$ , and dominated by  $R_{im}$ .

With the limiting condition that  $r_m > R_{2m}$ , a lower limit of 3 × 10<sup>3</sup> s<sup>-1</sup> is calculated for the solvent exchange rate at -45 °C in this system.

(28) For acetone as a  $\sigma$  type Lewis base, the C-O-M angle usually ranges from 120 to 150°. For example, see: Cotton, F. A.; Matusz, M. *Inorg. Chem.* **1987**, *26*, 3468. Galeffi, B.; Simard, M.; Wuest, J. D. *Ibid.* **1990**, *29*, 951.

(29) The Co-O bond length is taken as 2.3 Å from the Co-O bond length in Co(dmgBF<sub>2</sub>)<sub>2</sub>(CH<sub>3</sub>OH)<sub>2</sub> from ref 22.

(30) *Handbook of Chemistry and Physics*, 53rd ed.; CRC Press: Boca Raton, FL, 1972; F-37.

**Table 2.** Kinetic Parameters for Solvent Exchange of Cobaloxime(II) Solutions

complex	solvent	$\Delta H^\ddagger$ (kcal mol <sup>-1</sup> )	$\Delta S^\ddagger$ (cal mol <sup>-1</sup> K <sup>-1</sup> )	$k_{\text{obs}}$ (s <sup>-1</sup> , 25 °C)	$A/\hbar \times 10^6$ (s <sup>-1</sup> )
Co(dmgH) <sub>2</sub>	CH <sub>3</sub> CN	7.2 ± 0.2	-9.8 ± 0.7	2.3 × 10 <sup>5</sup>	-4.88
	CH <sub>3</sub> OH	13.9 ± 0.2	8.3 ± 0.6	2.8 × 10 <sup>4</sup>	+16 (CH <sub>3</sub> ), +15 (OH)
Co(dmgBF <sub>2</sub> ) <sub>2</sub>	CH <sub>3</sub> CN	4.3 ± 0.3	-20.5 ± 1	1.4 × 10 <sup>5</sup>	3.39
	acetone	3.4 ± 0.9	-22 ± 5	3.5 × 10 <sup>5</sup>	1.87
Co(dpgH) <sub>2</sub>	CH <sub>3</sub> CN			≥ 4 × 10 <sup>5</sup> <sup>b</sup>	
	CH <sub>3</sub> OH	3.4 ± 0.4	-21 ± 2	1.2 × 10 <sup>6</sup>	9.46
Co <sup>2+</sup>	CH <sub>3</sub> CN <sup>c</sup>	11.8	6.5	3.4 × 10 <sup>5</sup>	-0.14 <sup>d</sup>
	CH <sub>3</sub> OH <sup>c</sup>	13.8	7.2	1.8 × 10 <sup>4</sup>	+2.6 (CH <sub>3</sub> ), +5.0 (OH) <sup>e</sup>
Co( <i>trans</i> -[14]diene) <sup>2+</sup>	CH <sub>3</sub> CN <sup>f</sup>				-2.24
	CH <sub>3</sub> OH <sup>f</sup>				6.0 (OH)

<sup>a</sup> If the sign is not given, only the absolute value is known. <sup>b</sup> Estimated from the lower limit exchange rate constant of  $3 \times 10^3$  s<sup>-1</sup> at -45 °C (see text) with an assumed  $\Delta H^\ddagger$  value of 5 kcal mol<sup>-1</sup>. <sup>c</sup> Kinetic results from ref 31. <sup>d</sup> Reference 33. <sup>e</sup> Reference 34. <sup>f</sup> Reference 17.

**Co(dpgH)<sub>2</sub> in Methanol.** The experimental  $R_{ip}$  data are plotted in Figure 3, and the log  $R_{ip}$  plots are similar to those of Co(dmgBF<sub>2</sub>)<sub>2</sub> in acetonitrile and acetone in that the solvent exchange region is evident but is not well defined. The parallel dependence of  $R_{2p}$  and  $R_{1p}$  on temperature in region I indicates that  $E_{1m} \approx E_{2m}$ . The large difference between  $R_{2p}$  and  $R_{1p}$  can be attributed to the inner-sphere scalar relaxation contribution (eq 12).

The  $R_{ip}$  data were analyzed first by assuming  $C_{1m} = 0.5C_{1o}$ , as for Co(dmgH)<sub>2</sub> in CH<sub>3</sub>OH,  $E_{1m} = E_{2m} = E_{1o} = E_{2o}$ , and  $C_{1o} = C_{2o}$ . However, convergence of the least-squares fitting can only be obtained by fixing the  $C_{2m}$  value. For  $C_{2m}$  in the range 660–8000 s<sup>-1</sup> K, the least-squares fits have essentially the same variance. The lower limit of  $C_{2m}$  is set by the  $C_{1m}$  value which is half that of  $C_{1o}$ , while for  $C_{2m} > 8000$ , convergence could not be attained. The best-fit parameters corresponding to  $C_{2m}$  values of 660 and 8000, respectively, are both listed in Table 2, and the curves in Figure 3 were calculated by a set of parameters obtained from the fitting with a middle value of  $C_{2m} = 5000$ .

It can be seen in Table 1 that the  $E_{im}$ ,  $C_{1o}$  (and  $C_{1m}$ ) values are not sensitive to changes in the  $C_{2m}$  values, and two sets of  $\Delta H^\ddagger$ ,  $\Delta S^\ddagger$ , and  $C_w$  values obtained at the two limiting  $C_{2m}$  values are essentially equal within their error limits. The electron spin relaxation time  $T_e$  of  $7.9 \times 10^{-11}$  s calculated by using  $C_{2m} = 8000$  s<sup>-1</sup> K seems more reasonable since it is close to that of  $6.6 \times 10^{-11}$  s for Co(dmgH)<sub>2</sub>-CH<sub>3</sub>OH (Table 1). Thus,  $C_{2m}$  is probably closer to 8000 than to 660 s<sup>-1</sup> K.

## Discussion

The kinetic parameters for solvent exchange generally have been useful in quantifying the lability of the metal complex and in providing guidance to the mechanism for ligand substitution at the metal center. Such results for a number of first-row transition metal ions in the II and III oxidation states were reviewed and discussed recently. Merbach<sup>31</sup> used the activation volumes for such reactions to suggest a general shift from associative to dissociative activation with increasing atomic number and decreasing oxidation state for such systems. This trend also may be reflected in the activation entropies.<sup>32</sup>

The kinetic results from this study are summarized in Table 2. The low-spin d<sup>7</sup> cobaloximes(II) are quite labile species with solvent exchange rate constants in the range 10<sup>4</sup>–10<sup>6</sup> s<sup>-1</sup> (25 °C). These values are in the same range as those for hexasolvated, high-spin cobalt(II). The most remarkable factor about the cobaloximes(II) is the wide range of  $\Delta H^\ddagger$  and  $\Delta S^\ddagger$  values for different solvents and different oxime modifications. For example, in acetonitrile the  $\Delta H^\ddagger$  changes from 7.2 to 4.3 for

Co(dmgH)<sub>2</sub> and Co(dmgBF<sub>2</sub>)<sub>2</sub>, respectively. Similarly in methanol, the change is from 13.9 to 3.8 for Co(dmgH)<sub>2</sub> and Co(dpgH)<sub>2</sub>, respectively. These rather spectacular changes are counterbalanced by changes in  $\Delta S^\ddagger$  so that the rate constants at 25 °C are not greatly different. This behavior is typical of systems showing an isokinetic relationship, and eq 15 gives a

$$\Delta H^\ddagger = 301\Delta S^\ddagger + 9976 \quad (15)$$

reasonable representation of the results ( $r = 0.97$ ) with an isokinetic temperature of 301 K. The more surprising, and probably fortuitous, observation is that this correlation also includes the high-spin, hexasolvated cobalt(II) systems in water, methanol, acetonitrile, DMF, and ammonia.<sup>32</sup>

The interpretation of isokinetic relationships is fraught with controversy and may be attributed to anything from mechanistic trends to systematic experimental errors. If the former is accepted, and the positive  $\Delta S^\ddagger$  and  $\Delta V^\ddagger$  for the hexasolvated systems indicate an I<sub>d</sub> mechanism, then the negative  $\Delta S^\ddagger$  for some of the cobaloxime(II) systems implies a shift toward an I<sub>a</sub> mechanism. The electron-withdrawing -BF<sub>2</sub> substituents would be expected to favor an I<sub>a</sub> mechanism by enhancing bonding to the entering solvent nucleophile. This is consistent with the more negative  $\Delta S^\ddagger$  values compared to those for the Co(dmgH)<sub>2</sub> systems. However, electronic differences between the methyl and phenyl derivatives should be minor and would not seem to explain the very negative  $\Delta S^\ddagger$  for Co(dpgH)<sub>2</sub> in methanol. Steric effects might favor 5-coordination for Co(dpgH)<sub>2</sub> and an I<sub>a</sub> mechanism, but further speculation seems unwarranted.

The scalar coupling constant  $A/\hbar$  of five cobaloxime(II) systems are collected in Table 2 along with the values for Co(*trans*-[14]diene)<sup>2+</sup> and Co<sup>2+</sup> ions in acetonitrile and methanol. Among the cobaloxime(II) systems, the signs of the coupling constants are available only for Co(dmgH)<sub>2</sub> in acetonitrile and methanol, from the directly measured proton shifts in the fast-exchange limit. This information indicates the mechanism of delocalization of the unpaired electron spin density. The negative  $A/\hbar$  for the methyl protons of CH<sub>3</sub>CN is consistent with the negative scalar coupling constants observed for Co(*trans*-[14]diene)<sup>2+</sup>-CH<sub>3</sub>CN<sup>4</sup> and Co(CH<sub>3</sub>CN)<sub>6</sub><sup>2+</sup><sup>33</sup> and indicates a spin polarization mechanism. The positive  $A/\hbar$  values for CH<sub>3</sub> and OH protons indicate a direct transfer of unpaired spin from the cobalt 3d<sub>z<sup>2</sup></sub> orbital to the methanol oxygen orbital through the  $\sigma$  bond. From the oxygen, the spin density is then transferred to the OH proton, and to the CH<sub>3</sub> protons *via* the carbon sp<sup>3</sup> orbitals.<sup>34</sup> The direct spin transfer mechanism would cause an increase in positive spin density for both the CH<sub>3</sub> and OH protons, as reflected by the similar positive  $A/\hbar$  values for OH and CH<sub>3</sub> protons. The larger  $A/\hbar$  for OH relative to CH<sub>3</sub>

(31) Merbach, A. E. *Pure Appl. Chem.* **1987**, *59*, 161.

(32) Jordan, R. B. *Reaction Mechanisms of Inorganic and Organometallic Systems*; Oxford University Press: New York, 1991; Chapter 3.

(33) Matwijoff, N. A.; Hooker, S. V. *Inorg. Chem.* **1967**, *6*, 1127.

(34) Breivogel, F. W., Jr. *J. Chem. Phys.* **1969**, *51*, 445.

for  $\text{Co}(\text{CH}_3\text{OH})_6^{2+}$  has been interpreted as the direct spin transfer to the OH proton by overlap of the cobalt  $t_{2g}$  orbital and the hydrogen  $1s$  orbital.<sup>34</sup>

It is interesting to note that the  $|A/\hbar|$  values for the low-spin cobaloxime(II) complexes are 5–20 times larger than those for the high-spin hexasolvated species. In principle, this should be of benefit to NMR solvent exchange studies such as this by amplifying the  $(\Delta\omega_m)^2/r_m$  contribution (eq 7). Unfortunately,

this advantage is offset by the longer  $T_e$  values, which make the  $R_{2m}$  and  $R_{2o}$  values larger compared to those of the high-spin cobalt(II) systems.

**Acknowledgment.** The authors thank the Natural Sciences and Engineering Research Council of Canada for support for this work.

IC950201H